



ELSEVIER

Available online at www.sciencedirect.com

SCIENCE @ DIRECT®

Surface and Coatings Technology 172 (2003) 204–216

**SURFACE
& COATINGS
TECHNOLOGY**

www.elsevier.com/locate/surfcoat

Contact fatigue failure modes in hot isostatically pressed WC-12%Co coatings

S. Stewart, R. Ahmed*

Heriot-Watt University, School of Engineering and Physical Sciences, James Naysmith Building, Riccarton, Edinburgh EH14 4AS, UK

Received 17 September 2002; accepted in revised form 19 February 2003

Abstract

The objective of this experimental study was to investigate the influence of the post-treatment, Hot Isostatic Pressing (HIPing), on the Rolling Contact Fatigue (RCF) performance of thermal spray (WC-12%Co) coatings. Thermal spray coatings were deposited using a JP5000 High Velocity Oxy Fuel (HVOF) system in three different thicknesses on the surface of 440-C steel substrate cones to vary the depth of the shear stress within the Hertzian stress field. The furnace temperature during the HIPing process was varied at 850 °C and 1200 °C. RCF tests were conducted using a modified four ball machine under identical tribological conditions of contact stress, configuration and lubrication. Surface observations were made using Scanning Electron Microscopy (SEM) and Light Microscopy. Results of this preliminary study, which is the first of its kind in published literature to evaluate the RCF of HIPed cermet coatings, indicate that variation in HIPing temperature can have a significant influence on a coating's delamination resistance. These results are discussed to comprehend the performance and ascertain the fatigue failure modes in HIPed HVOF coated rolling elements. Apart from comparing the failure modes between HIPed and As-Sprayed coatings, results indicate that by increasing the HIPing temperature to 1200 °C, and maintaining full film lubrication, it is possible to achieve a fatigue life in excess of 70 million stress cycles without failure in relatively thin (50 μm) cermet coatings. Coating failure was attributed to maximum shear stress occurring either at the coating/substrate interface or within the coating microstructure, resulting in delamination due to cyclic loading.

© 2003 Elsevier Science B.V. All rights reserved.

Keywords: Thermal spray; Hot isostatic pressing; Rolling contact fatigue; Failure modes

1. Introduction

Thermal spray cermet coatings deposited by techniques such as detonation gun, HVOF and arc-wire are used in many industrial applications ranging from aerospace to the biomedical industry for applications requiring abrasion, sliding, fretting and erosion resistance. This is because the hard WC particles form the major wear resistant constituent of the material whilst the cobalt binder provides toughness and support. Properties such as hardness, wear resistance and strength are influenced primarily by the WC grain size and volume fraction and in the case of thermally sprayed WC coatings also varying the porosity, carbide and binder phase composition.

Rolling Contact Fatigue (RCF) is responsible for the fatigue failure of rolling element bearings, gears, camshafts and may be defined as cracking or pitting/delamination limited to the near surface layers of bodies in rolling/sliding contact. There is an increased demand for improved lifetime reliability and load bearing capacity of bearing materials and future applications call for their use in more hostile environments.

Since thermal spray coatings can provide a cost-effective solution for tribological applications in rolling/sliding contact, a number of investigations have been carried out on the durability of these coatings in rolling/sliding contact. A combination of parameters has been shown to dictate the performance of these coatings. These parameters have been identified as coating porosity, substrate material, coating thickness, choice of lubricant, residual stresses and adhesion strength of the coating to the substrate. By optimising these parameters

*Corresponding author. Tel.: +44-131-449-5111; fax: +44-131-451-3129.

E-mail address: r.ahmed@hw.ac.uk (R. Ahmed).

it is possible to greatly improve the performance of these coatings in rolling/sliding contact. Hence, the industrial application of WC-Co coatings in Hertzian loading conditions can bring significant economic gain to the thermal spray industry.

1.1. Previous RCF studies

Investigations into the rolling contact fatigue behavior of thermal spray coatings were performed by Tobe et al. [1] and observed that surface roughness was highly influential in the fatigue performance. Later studies by Tobe et al. [2] on aluminum substrate revealed that shear stress between the coating and substrate were the most important factors for the RCF performance of these coatings. Following on from this investigation, Sahoo [3] studied the RCF resistance of WC-Co coatings in high stress applications and concluded that cracks initiated from the surface and propagated through the coating. Meanwhile, a study on detonation gun coatings by Hadfield et al. [4] concluded that WC-Co coatings failed within the microstructure. Yoshida et al. [5] also observed that the performance of WC-Co coatings in rolling/sliding contact was influenced by the coating thickness whereby thinner coatings showed low fatigue life if the substrate surface was not shot blasted prior to coating.

Using this knowledge, Ahmed and Hadfield [6] investigated the RCF performance of WC-Co coatings deposited by a super detonation gun. From the experimental results it was concluded that edge cracks could have initiated failure on the surface of the coatings and that delamination occurred through the coating itself but failure did not occur at the coating/substrate interface. FEM analysis indicated that variation of the coating thickness altered the location rather than the magnitude of the shear stresses within the coating. More recent investigations by Ahmed et al. [7] involved studying the RCF performance of WC-Co coatings deposited by the HVOF process. The rolling elements were coated in three different coating thicknesses and three different lubricants were incorporated in order to assess the performance of the coatings under various tribological conditions. Results showed that under full film lubrication, a thin coating (20 μm thickness) displayed superior performance. This was because the location of maximum shear stress was within the substrate. When coating thickness was increased there was a shift in the depth of shear stress reversal into the coating microstructure and hence failure was from a combination of surface wear and sub surface delamination. Therefore, variation in RCF performance was attributed to the effects of film thickness and variations in the location of maximum shear stress.

Ahmed et al. [8] also investigated the generation of residual stresses in thermal sprayed coatings using a

non-destructive experimental approach, X-ray diffraction. Residual stresses were analysed in RCF tested balls and cones of various coating thicknesses. Variation in RCF tests involved change in lubricant and also the type of planetary balls (steel, ceramic). The conclusions from this analysis were that residual stress attenuation was higher in the near surface layer of the wear track than in the direction of rolling. The failed coating area displayed low compressive residual stress indicating high relaxation of compressive residual stress during the coating fracture. The residual stress values in the rolling elements changed with the direction of stress measurement and with the change in substrate geometry.

Based on this knowledge of residual stresses within RCF tested thermal spray coatings, further analysis was carried out on the failure modes of RCF tested HVOF thermal spray coatings [9]. From this investigation, results from RCF testing showed that by control of the coating thickness, residual stress and tribological conditions of contact stress and lubrication regime, it was possible to achieve a fatigue life in excess of 70 million stress cycles without failure. A new failure mode was also observed in the coatings and was termed spalling because of its resemblance to spalling failure in conventional bearings. This failure mode was attributed to improved fracture toughness and a higher level of compressive residual stresses within the coating.

1.2. Hot isostatic processing

It is generally accepted that the microstructure of thermal spray coatings is highly dependant on the spraying method and the parameters associated with spraying such as particle size, type of powder used, velocity of spray, etc. The porosity and secondary phase particles in the coating normally lead to stress concentrations within the microstructure. It is a well-established fact that the brittleness and weakness of sprayed coatings are due to their lamellar structure where individual lamellae's do not adhere to one another completely. Hence the use of these coatings is limited to low stress applications. Voort [10] initially showed that thermal spray coatings not only contain significant porosity but also secondary phase particles and lack of fusion. The delamination failure is therefore a result of three effects: lamella structure, porosity and secondary phase particles.

The search for coatings which are able to withstand the harsh conditions of modern-day industrial applications has led to the study of post-treated (Hot Isostatically Pressed) hard cermet coatings. Hot Isostatic Pressing (HIPing) is a post treatment application which involves placing batches of coated samples inside a furnace which is contained within a pressure vessel. The coated samples are normally encapsulated in order to prevent surface cracking which can result in the harsh conditions imposed by HIPing. However, this safety

precaution restricts the shape and size of samples. Since emphasis in thermal spray research is to continually search for cost effective and reliable solutions, in this current study the coated samples were HIPed without encapsulation.

The published literature on investigations into post-treated thermal spray coatings is limited. Ito et al. [11] investigated the microstructure and wear resistance of plasma sprayed WC-Co coatings which were HIPed in the temperature range of 873 to 1273 K and the pressure range of 0.9 to 5 MPa [11]. Wear tests were carried out using an abrasive wear tester. Results from the experimental analysis concluded that pores in the microstructure of the as-sprayed coatings were appreciably reduced when HIPing was carried out at temperatures above 973 K (600 °C). Hardness of the coating increased after HIPing and wear resistance was significantly improved. The relative increase in coating hardness was related to densification within the coating which is a result of the high pressure and temperature during HIPing. Wear resistance improved due to a combined effect of increased coating hardness and also improved adhesion at the coating/substrate interface was observed. The absence of pores in the coating would significantly alter the magnitude and location of quenching (residual) stresses within the coating since residual stresses are extremely sensitive to changes within the coating microstructure as shown in investigations by Ahmed et al. [8]. Hence, delamination failure in rolling contact fatigue can be related to porosity within the microstructure as well as stress concentrations resulting from poor lamellae structure.

Later studies by Khor et al. [12] who investigated the effect of HIPing on plasma sprayed nickel based coatings verified these initial findings. In this study Ni–Al coatings were deposited on medium carbon steel substrate which had been grit blasted. A number of HIPing cycles were performed on the coatings. The HIPing temperature range was in the condition of 750–950 °C whilst the pressure was varied from 50 to 200 MPa. Holding time was kept constant for 1 h. Results from the microstructural analysis and microhardness measurements found that after HIPing, there was a significant reduction in porosity level with a related increase in hardness. It was also noted that these effects were more apparent at higher HIPing pressures.

A more detailed investigation on the changes in coating microstructure after HIPing was carried out by Chen et al. [13]. Plasma sprayed ZrO₂ coatings were deposited onto cold mild steel substrate forming a coating thickness of 300 μm. The coating was HIPed in argon environment at 1250 °C. The pressure was 200 MPa which was held for 8 h. Results from a detailed microstructural analysis observed that after HIPing coatings displayed a dense and crackless microstructure. The interlamellar porosity was completely eliminated whilst

the spherical pores changed into microvoids less than 0.1 μm in size. Also, the microstructure has lost all its lamellar morphology. Similarly, under high magnification it was observed that under long exposure at elevated temperatures and high isostatic pressure, columnar grain growth and recrystallization occurred.

The effect of pore size distribution after HIPing was studied in detail by Khor [14] using Plasma Sprayed coatings. Zirconia based coatings were deposited on medium carbon steel substrate. A number of HIPing cycles were undertaken in order to ascertain the degree of sensitivity on the HIPing conditions with respect to the mechanical properties of the coating. The furnace temperature was varied between 900 °C and 1200 °C whilst the operating pressure was kept constant at 180 MPa. The holding time was either 1 or 3 h. From microstructural analysis, observations showed a lower incidence of pores and relatively improved inter-lamellar adhesion. There was no evidence of any grain growth in samples HIPed for 1 h. However, samples HIPed for duration of 3 h did show evidence of grain growth. It was deduced that HIPing of 3 h might have caused the open pore channels to enlarge since the coatings were HIPed without encapsulation and pores were subjected to high isostatic pressure. Hence, it was concluded from both microstructural analysis and microhardness measurements that beyond HIPing treatment of 1 h, the physical response of the coating appeared to be insensitive to HIPing temperature.

Recently Khor et al. [15] have performed further investigations on the effect of HIPing plasma sprayed coatings. The number of HIPing cycles in this investigation was reduced. Pressure and time were kept constant at 180 MPa and 1 h, respectively, whilst the temperature was varied in the range of 1000 to 1200 °C. Results from microstructural analysis observed no evidence of any grain growth in the HIPed samples. The reduction in porosity was found to be less significant in this investigation, however, micro hardness results indicated a noticeable increase in hardness after HIPing. This result was attributed to a reduction in fine pores which were 0.2 μm in diameter.

It is important to investigate the durability of HIPed thermal spray coatings in rolling/sliding contact. Previous investigations on HIPed coatings indicate that significant improvement in the coating microstructure can be achieved by HIPing yet, to date no investigation to study the performance or failure modes of HIPed thermal spray coatings exist in published literature.

This preliminary study hence marks the first investigation in published literature, in which the fatigue of HIPed thermal sprayed WC-Co coatings were studied in rolling/sliding contact under constant tribological conditions of contact configuration for different coating thicknesses under fully developed lubrication regime.

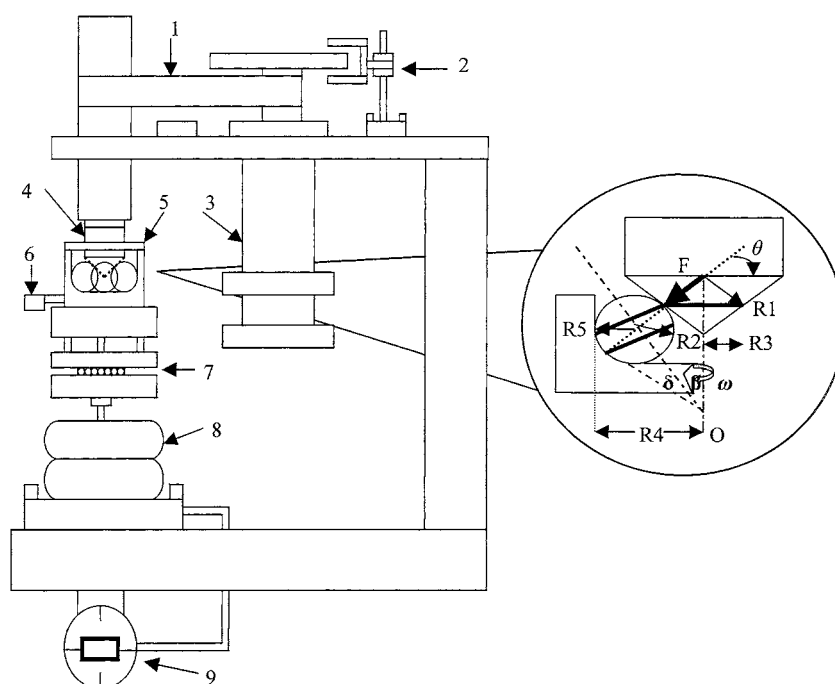


Fig. 1. Schematic of the modified four-ball machine. ($R_1=R_2=6.35$ mm, $R_3=3.65$ mm, $R_4=14.2$ mm, $R_5=7.62$ mm, $\theta=35.15^\circ$, $\beta=29.52^\circ$, $\delta=25.33^\circ$, $\omega=4000\pm 10$ rpm). (1, Belt drive; 2, speed sensor; 3, Spindle driving motor; 4, coated cone and collet; 5, cup assembly; 6, Thermocouple; 7, thrust bearing; 8, bellows; 9, Pressure Gauge).

Prior to this study, WC-Co thermal spray cones were HIPed under the condition of the temperature range from 850 to 1200 °C and the pressure of 100 MPa. A modified four-ball machine which differs from the four-ball machine, in the sense that lower planetary balls are free to rotate, was used to investigate the rolling contact fatigue performance. The failed rolling element coatings are analysed for surface failures using SEM observations. The results are discussed with the help of microhardness and measurements and elastic modulus analysis.

2. Experimental test procedure

2.1. Test configuration

A modified four-ball machine was used to study the RCF performance of HIPed thermal spray rolling elements (Fig. 1). This machine simulates the configuration of a deep groove rolling element ball bearing. It was used as an accelerated method for the evaluation of RCF performance as many more stress cycles can be achieved in a fixed contact area. The coated rolling element cone was assembled to the drive shaft via a collet and drove the three planetary balls which act as the rolling elements in the configuration of the deep groove ball bearing. The stationary cup represents the outer race of the rolling element ball bearing in the contact model of the modified four-ball machine.

The cup assembly was loaded via a pneumatic piston below the steel cup to generate the required Hertz contact stresses between the coated rolling element and the planetary balls. Conventional cleaning methods were used to avoid contamination of the contacting surfaces in the cup assembly before the RCF tests. The tests were conducted at an ambient temperature of approximately 25 °C. The spindle speed was set to 4000 ± 5 rpm using a high speed drive. The machine was set to stop at the onset of failure in the cup assembly, i.e. when the vibration amplitude increased to a value above the preset level.

The cup assembly was of type II [16] having a surface hardness of 60 HRC (Hardness Rockwell C). RCF tests were conducted in conventional steel ball bearings (steel planetary balls) which were grade 10 carbon chromium steel with an average surface roughness (R_a) of 0.02 μm .

2.2. Coated cone test elements

A liquid fuel HVOF (JP5000) system was used to deposit WC-12%Co coatings on the surface of 440-C rolling element cones. This system was selected because of its higher particle velocities, which are in the range of 1,005 to 1,118 m/s, and a more uniform distribution of particles within the spray stream, resulting in better coating quality. The coating and substrate materials were selected because of their desired synergy of mechanical

Table 1
Properties of test lubricant

Lubricant type (c.s. °C)	Specific gravity at 15 °C	Flash point (°C)	Pour point (°C)	Kinematic viscosity (c.s. °C)	
				40 °C	100 °C
Hitec-174	0.95	255	−20	200	40

and thermal properties. The substrate rolling element cones were 14.5 mm in diameter and had an apex angle of 109.4 degrees. The substrate material was sand-blasted prior to the coating process to improve the adhesive strength due to the increased bonding contact area and the mechanical interlock between the coating and substrate material. The rolling elements were coated in three thicknesses by several passes of spraying, in a direction perpendicular to the cone axis. The rolling elements were then ground and polished to give an average coating thickness of 250, 150 and 50 µm. The cones were then HIPed at two different furnace temperatures of 850 °C and 1200 °C in unencapsulated conditions. Choice of HIPing temperature was based on the premise that the lower temperature would give minimum distortion to the substrate material, whilst the higher temperature would be beneficial for the microstructural transformation of the coating material. This is consistent with the findings by Nerz et al. [17] where exothermic reactions relating to microstructure changes were reported at approximately 850 °C. The heating and cooling rate for both cycles was kept constant at 8 °C/min in order to prevent surface cracking. A constant pressure of 100 MPa on the samples was maintained for 1 h by argon gas being pressurised against the surface of the

cones. Under these conditions none of the coatings exhibited any signs of cracking.

2.3. Test conditions

The purpose of this study was to ascertain any improvements in the coatings during rolling/sliding contact after the post-treatment HIPing, therefore, tests were conducted exactly under the same tribological conditions of Hertzian contact stress and contact configuration. A high viscosity lubricant, Hitec 174, was used in all of the tests. The Elasto-Hydrodynamic Lubrication (EHL) results have been calculated in previous investigations [9] and indicated full film regime. The chemical properties of the lubricant are shown in Table 1. Table 2 summarises the RCF results. These results are not intended for statistical fatigue life prediction, but to understand the performance of coated cones in RCF tests under various HIPing conditions. The peak compressive stress values listed in Table 2 were based upon the uncoated case of the contacting rolling elements. The stress values were calculated using the following relationship:

$$P_o = \frac{3F}{2\pi ab} \quad (1)$$

Table 2

Rolling contact fatigue tests for as-sprayed, HIPing at 850 °C and HIPing at 1200 °C HVOF coated rolling elements on bearing steel (440-C) substrate

Test no	Coating thickness (µm)	Contact load (F) (N)*	Planetary balls	Contact stress (Po) (GPa)*	Contact width (b) (mm)	Depth of Max: shear (Y=0.65b)* (µm)	Test lubricant	Maximum lubricant temperature (°C)	No of stress cycles (millions)	Failure type
As-sprayed tests										
T1	50	380	Steel	2.7	0.13	85	Hitec 174	37	1	Delamination
T2	150	380	Steel	2.7	0.13	85	Hitec 174	36	55	None [▲]
T3	250	380	Steel	2.7	0.13	85	Hitec 174	29	70	None [▲]
HIPed at 850 °C tests										
T4	50	380	Steel	2.7	0.13	85	Hitec 174	25	0	Delamination
T5	150	380	Steel	2.7	0.13	85	Hitec 174	36	27	Delamination
T6	250	380	Steel	2.7	0.13	85	Hitec 174	32	29	Delamination
HIPed at 1200 °C tests										
T7	50	380	Steel	2.7	0.13	85	Hitec 174	33	70	None [▲]
T8	150	380	Steel	2.7	0.13	85	Hitec 174	31	70	Denting/SD
T9	250	380	Steel	2.7	0.13	85	Hitec 174	34	70	None [▲]

SD = Surface Distress.

* Values calculated for uncoated case.

▲ Suspended test after 55–70 million stress cycles.

Table 3
Hardness results for as-sprayed, HIPed at 850 °C and HIPed at 1200 °C coatings

Hardness HV, measurement area	WC-12Co as-sprayed	WC-12Co HIPed at 850 °C	WC-12Co HIPed at 1200 °C
Surface	1320	1642	1722
Cross section (50 μm)	1424	1677	1785
Cross section (100 μm)	1568	1631	1802

Table 4
Elastic modulus results for as-sprayed and HIPed coatings

Elastic Modulus GPa, measurement area	WC-12Co as-sprayed	WC-12Co HIPed
Surface	231	247
Cross section (50 μm)	183	300
Cross section (100 μm)	197	302

where ‘*a*’ and ‘*b*’ are the major and minor axis of Hertzian contact ellipse, which can be calculated from the geometrical dimensions and the values of Young’s modulus and Poisson’s ratio of the contacting rolling elements. The depth of maximum shear stress (τ_{\max}) included in Table 2 was evaluated using the conventional

contact mechanics approach reproduced here for clarity:

$$\tau_{\max} = 0.35 \times P_o \quad \text{at a depth of } 0.65b \quad (2)$$

3. Results

3.1. Surface observations

Post-analysis of the wear tracks using SEM and light microscopy displayed some interesting features. In Fig. 2 the wear track of the as-sprayed rolling element T2 is highlighted. No area of failure was observed. In Fig. 3 the wear track of the as-sprayed rolling element T3 was observed in greater detail using SEM. Fig. 4 and Fig. 5 displays the wear track of the rolling element T4. The coated rolling element was HIPed at 850 °C. An area of failure can be seen on the part of the wear track. Fig. 6 display the wear track of rolling element T6. Similar to the rolling element T5, the area of failure which was formed on part of the wear track has spread out with the confines of the wear track. In Fig. 7 and Fig. 8 the area of failure is shown in greater detail. No failure area was seen on the wear track of rolling element T7 (Fig. 9). However under higher magnification, evidence of abrasive pitting was seen within the wear track (Fig.

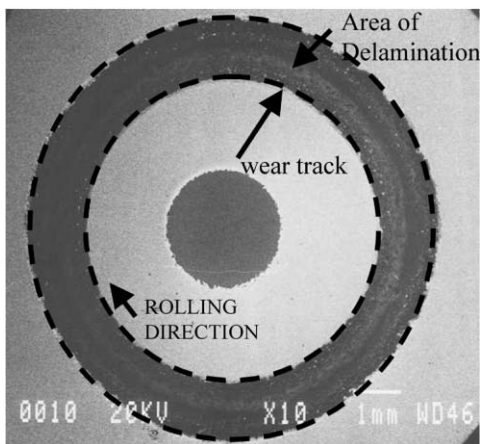


Fig. 2. Wear track after test T2.

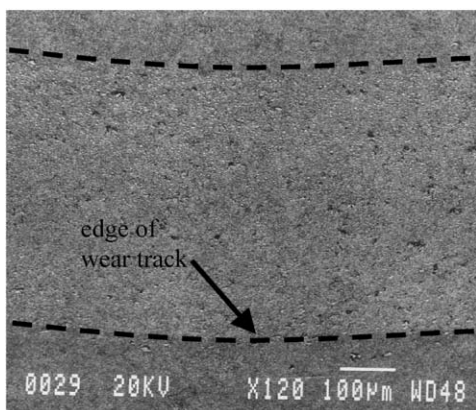


Fig. 3. Wear track after test T3.

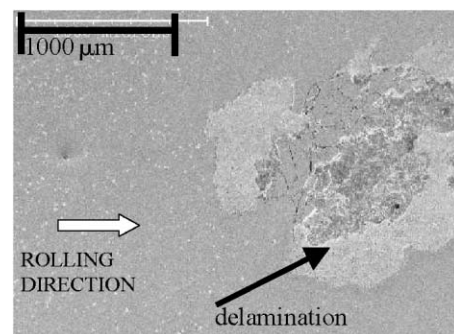


Fig. 4. Delamination on wear track T4.

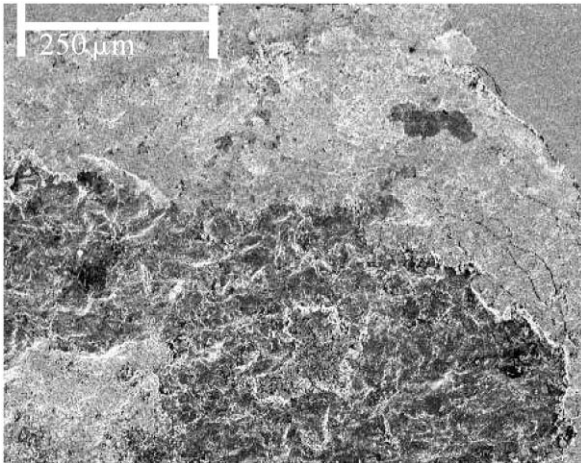


Fig. 5. Delamination on wear track T4.

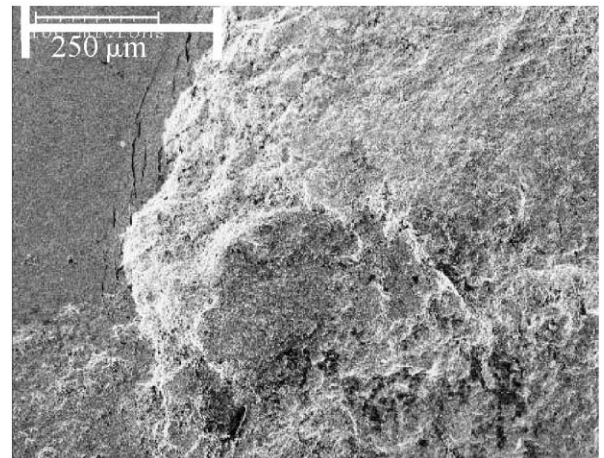


Fig. 8. Delamination on wear track T6.

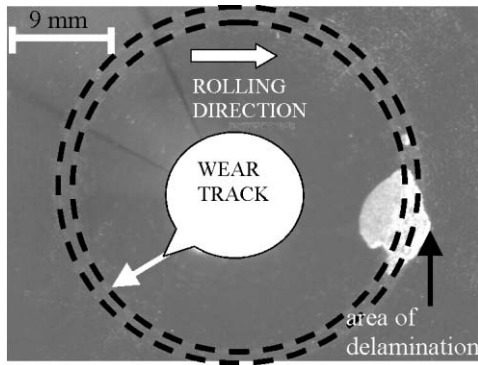


Fig. 6. Wear track after test T6.

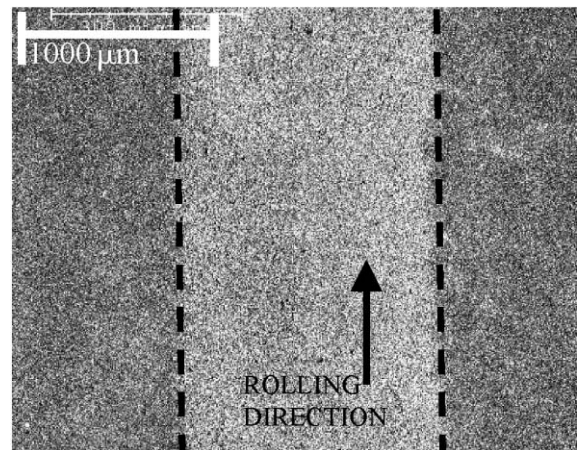


Fig. 9. Wear track after test T7.

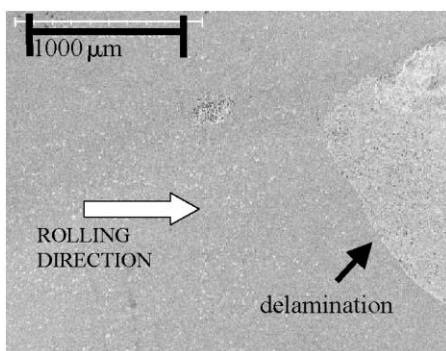


Fig. 7. Delamination on wear track T6.

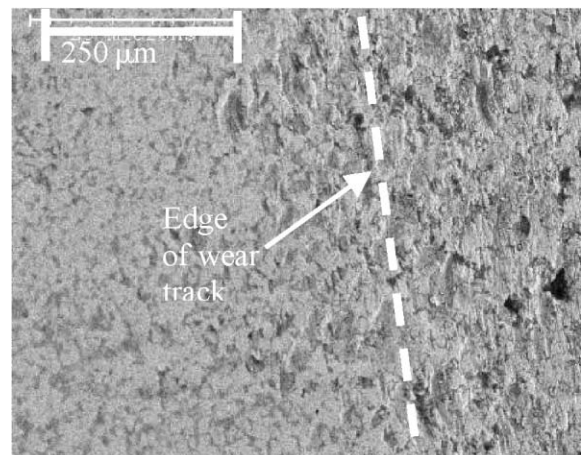


Fig. 10. Wear track after test T7.

10). This is termed surface distress and is identified by a number of microspalls which run together in a rough pebbly surface. In Fig. 11 a number of dents can be seen on the wear track. They are identified by a characteristic paddle shape, with an extending narrow neck. Surrounding the dents is evidence of localised surface distress, which is identified by a high frequency

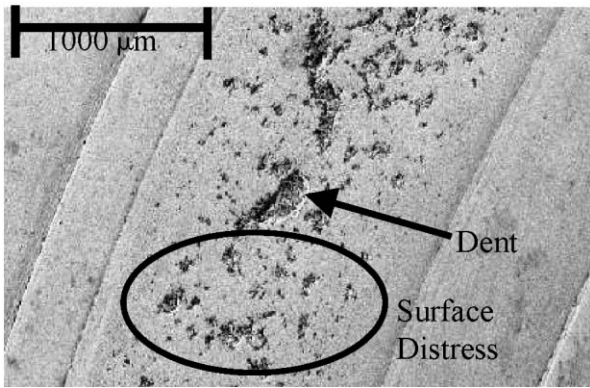


Fig. 11. Surface abrasion on wear track T8.

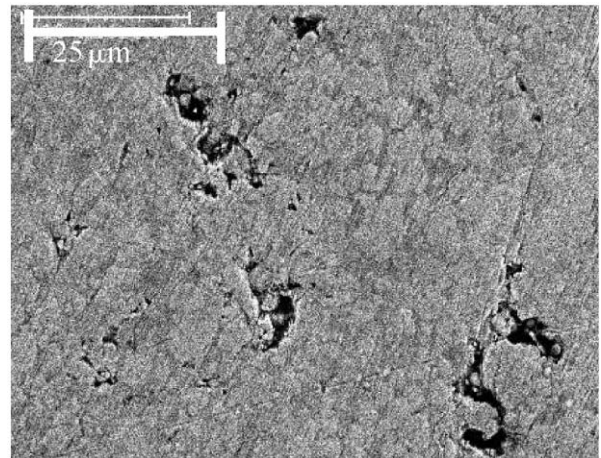


Fig. 14. Microstructure of T3.

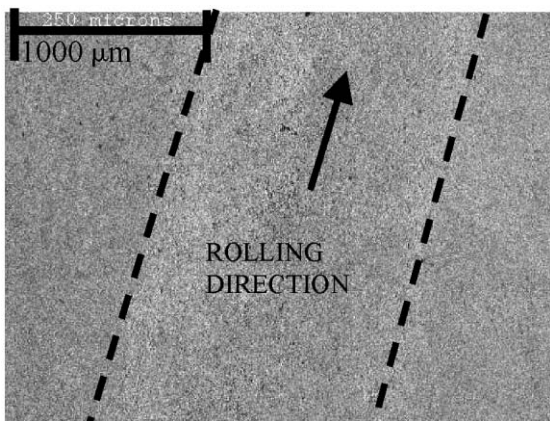


Fig. 12. Wear track after test T9.

of small shallow craters which are a result of asperity contact. Evidence of surface distress within the wear track can also be seen in Figs. 12 and 13 which shows

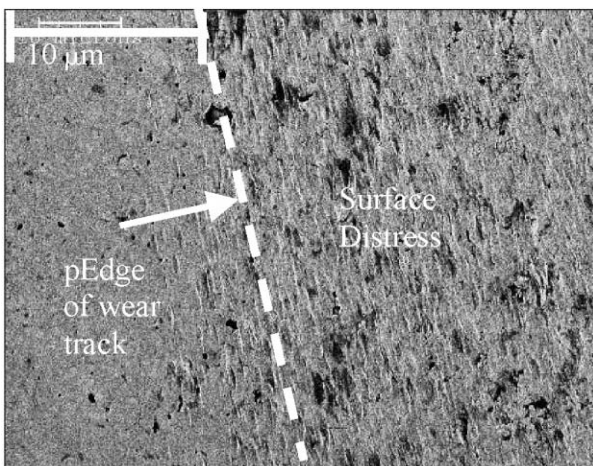


Fig. 13. Wear track after test T9.

the wear track of T9 at higher magnification and is similar to the wear track of T7.

3.2. Subsurface investigations

Sub-surface observation of coated rolling elements is critical in identifying the crack propagation within the coating microstructure or at the coating substrate interface, during tribological failure. The cross sections of the RCF tested cones were thus studied in detail using SEM in order to identify characteristics within the microstructure. Fig. 14 shows the microstructure of the as-sprayed coated rolling element T3. A number of micro-pits are visible within the microstructure and the carbides are on average round in shape. Fig. 15 shows the sub-surface observation of the coated rolling element T5 which was HIPed at 850 °C. A number of spherical pores are observed within the microstructure which were not observed in the as-sprayed coating. Fig. 16 displays

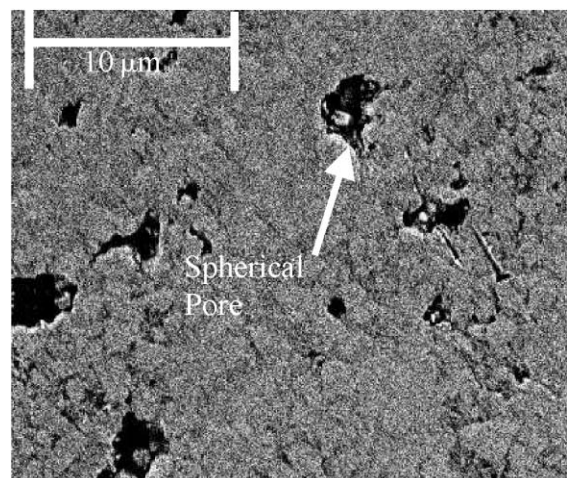


Fig. 15. Microstructure of T5.

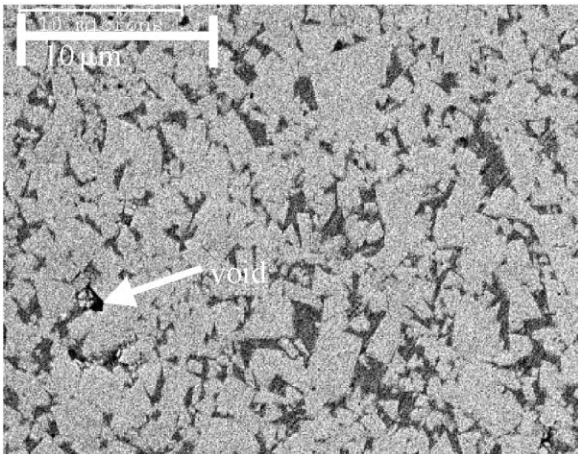


Fig. 16. Microstructure of T8.

the microstructure of the coated rolling element T8 which was HIPed at 1200 °C. The microstructure has lost all of its lamellar or splat morphology and densification has increased considerably with only a small frequency of microvoids appearing within the microstructure.

It was important to study the effect of HIPing on the coating/substrate interface. Fig. 17 shows the cross section of the as-sprayed rolling element cone T1. A definite interfacial line can be seen between the coating and the substrate which is a result of shot blasting the surface of the substrate prior to thermal spraying. At HIPing temperatures of 850 °C the interfacial line still exists (Fig. 18). However, the coating/substrate interface at elevated HIPing temperatures has changed considerably (Fig. 19). No interfacial line can now be seen as a result of inter-diffusion between the coating and the

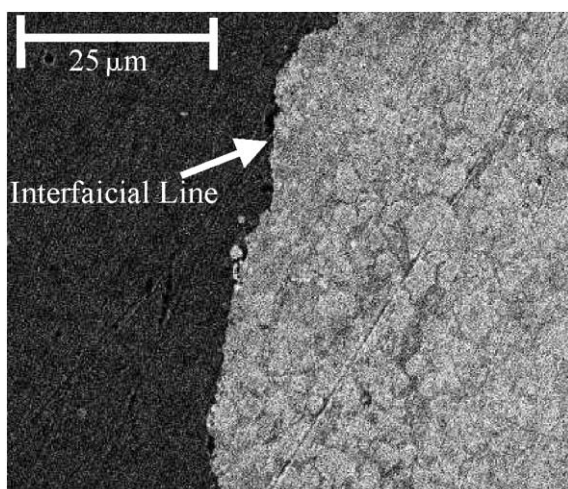


Fig. 17. Interface of As-Sprayed Coating.

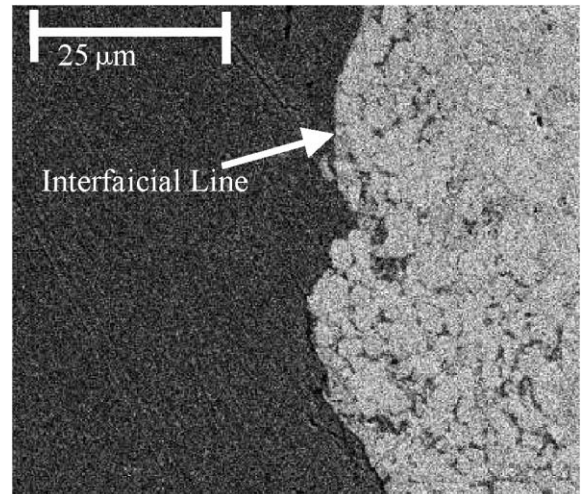


Fig. 18. Coating/substrate interface of T5.

substrate. A number of pores have appeared within the substrate, close to the interface. These pores are Kirkendall voids which are related to the diffusion process. The Kirkendall effect was cited in earlier investigations on diffusion of coatings by Dunand [18]. It gives the names to these pores and describes the phenomenon caused by two chemical species (coating, substrate) diffusing in opposite directions at different rates

3.3. Micro-hardness measurements

Hardness and Elastic Modulus measurements were performed on the as-sprayed and HIPed thermal spray coatings and were obtained using a nano indentation system. This system utilises a pendulum-based depth sensing equipment which was pivoted on frictionless

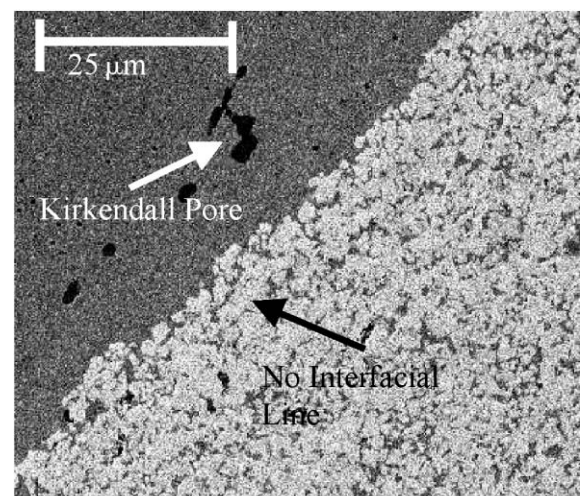


Fig. 19. Coating/substrate interface of T8.

bearings. A coil is mounted at the top of the pendulum. When an electric current is passed through the coil, the coil is attracted to a permanent magnet which results in the motion of the diamond indenter towards the coating and into the surface. Raw data are compiled initially from the rate of loading/unloading during the formation of each indentation. The depth vs. load raw data are then fitted to a power law function, originally proposed by Oliver and Pharr [19], to determine the hardness and elastic modulus values. Results are shown in Table 3 and Table 4. Hardness measurements were taken on the coating surface at a test load of 1000 mN and on the cross section of the coating at 500 mN. Results from the hardness measurements of the as-sprayed coating show an average value of 1320 HV. This compares well with previous investigations which give a value of 1318 HV [7] for identical coatings. In comparison, results from the surface of coatings HIPed at 850 °C displayed an average value of 1642 HV. This can be attributed to densification occurring within the coating during HIPing. At higher HIPing temperatures of 1200 °C the hardness of the coating surface was on average 1722 HV.

Studies were also performed to investigate any difference in the values of micro hardness on the surface and the coating cross-section due to the lamellar structure and anisotropy. Results from the cross-section analysis of the as-sprayed coating were slightly higher than the surface values and were observed to increase with increasing coating depth. However, cross-sectional analysis of the HIPed coatings showed no change in hardness results with increasing coating depth.

Elastic modulus measurements were taken on the surface of both as-sprayed and HIPed coatings (Table 4). Results from the surface of the as-sprayed coating show an average value of 231 GPa whilst results from the HIPed coatings display an average value of 247 GPa. Cross-sectional analysis of the as-sprayed coating showed a decrease in elastic modulus away from the surface, however, in contrast, the cross-sectional analysis of the HIPed coating displayed a relative increase in elastic modulus when measurements were moved from the surface and into the microstructure. This is an encouraging result since it indicates evidence of improved bonding mechanism.

4. Discussion

4.1. Failure modes

Classification of failure modes was made on the basis of surface and sub-surface observations of the failed rolling elements. Since the modified four-ball machine runs at high speed, it is difficult to observe crack propagation. Post-test examination is the only method

to ascertain failure modes and mechanisms. The principal aim of the current study was to ascertain whether similar failure modes occurred in post-treated coatings as had been previously seen in as-sprayed thermal spray coatings. Classification of failure modes in thermal spray coatings have been categorised into four main modes and named as abrasion, delamination, bulk failure and spalling [9]. However as seen in Table 2 only three modes of failure were identified in post-testing analysis. They were delamination, denting and surface distress.

Suh initially proposed a delamination theory of sliding wear in 1973. Suh [20], Flemming and Suh [21], Suh and Saka [22] and Suh [23] have since performed experimental and theoretical analysis supporting the delamination theory. The mechanism of delamination wear includes the propagation of cracks parallel to the surface at a depth governed by material properties and friction coefficient. Although rolling friction prevails in modified four ball tests and delamination theory is based on sliding friction, the results are still compelling. Damage theory of materials begins with the premise that material contains a multitude of defects in the form of microvoids [24] which undergo extension due to loading and unloading. A similar approach is adapted to explain the mechanism of coating delamination. The coating microstructure contains varying levels of micropores, micro-cracks and secondary phase particles, which acts as stress concentration points during cyclic loading.

Denting has been defined by Tallian [25] as a plastic depression (short gash, round edge, single or multifaceted impression, depressed solid or stripped line) caused in a working surface by a relatively incompressible object pressed into it by the passage of a contacting rolling element. Denting is the process by which dents form and is the result of a plastic impression made on a surface when a sharp asperity or entrapped foreign body is pressed into the contact surface under normal load. It is most distinct on rolling contact surfaces where the relative motion in the contact is predominantly normal to the surface.

Surface distress is defined by Tallian [25] as micro-scale spalling fatigue. It is failure on the wear track of rolling contact surfaces resulting in asperity scale microspall craters. The failure process involves two surfaces which are in predominant rolling contact under load and with lubrication. Their asperities approach each other in a direction close to the surface normal. Depending on the lubricant layer, stress substantially exceeding the macroscopic local Hertzian stress may develop in asperity encounters. Surface distress is therefore a result of decreasing EHL film thickness and also the height and sharpness of the surface asperities. It is identified by a rough surface within the wear track with a high

frequency of craters, which have a relatively shallow depth.

4.2. As-sprayed coated rolling elements

Results from the RCF testing of the as-sprayed coatings indicated that only T1 was stopped prematurely due to failure (Table 2). The thickness of the coating was 50 μm . From surface analysis, the failure mode was determined as delamination. Sub-surface analysis of the coating displayed substantial porosity within the microstructure (Fig. 14). The coating thickness was such that the coating/substrate interface was at the location of maximum shear stress. It is likely that delamination was a result of the location of the shear stress in this test accelerating crack propagation as a result of mismatch between the coating and substrate properties. Hence, during cyclic loading these cracks would have propagated to the surface and formed the area of failure. In tests T2 and T3 the depth of maximum shear stress was moved away from the coating/substrate interface due to increased coating thickness. Crack propagation was suppressed and hence failure did not occur at this level of Hertzian contact stress.

4.3. HIPed at 850 °C coated rolling elements

All tests on the coating, HIPed at 850 °C were prematurely terminated as a result of surface failure (Table 2). From surface analysis it was observed that failure was by delamination since the area of failure has spread beyond the width of the wear track (Figs. 4–8). Cross-sectional analysis of the coating indicated relatively high porosity within the microstructure (Fig. 15) and like the as-sprayed coating, (Fig. 17) there was no evidence of diffusion into the coating microstructure which has been shown to occur after HIPing [13]. There was also no evidence of recrystallization or interlamellar bonding.

In test T4 where the coating thickness was again such that the coating/substrate interface was at the location of the maximum shear stress it is likely that failure occurred for the same reasons as the as-sprayed coating of identical thickness, since no improvement in the microstructure was observed after HIPing.

In tests T5 and T6 the location of the maximum shear stress was moved away from the coating/substrate interface, however, failure was still shown to occur by delamination and after a relatively small number of stress cycles. In comparing the microstructure of the as-sprayed coatings (Fig. 15) and coatings HIPed at 850 °C (Fig. 16), it can be seen that the pores in the HIPed coating are in general slightly greater in size. Pores in thermal spray coatings can arise from the expansion of trapped gases. These pores are normally spherical in shape. HIPing has been shown in previous investigations

to remove these pores by a complex process [13]. HIPing leads to hot plastic deformation which causes the columnar grains to be broken into pieces forming many substructures and crystal defects within the grains. At elevated temperatures recrystallization takes place in these regions which contain substructures and crystal defects decreasing the system energy. After grain refinement either by static or dynamic recrystallization the newly formed equiaxed grains are very small due to incomplete grain growth. Under high isostatic pressure for at least an hour these grains will be compressed thus eliminating the pores. It is highly likely that the HIPing temperature of 850 °C was not high enough to cause this microstructural change, but instead the entrapped gases within the pores caused crack propagation to occur at the edges of these pores. During RCF testing, these pores and cracks at the edges of the pores would have acted as stress concentration points when combined with cyclic stresses which leads to failure by delamination.

From microhardness measurements it was shown that the hardness of the coating HIPed at 850 °C was significantly greater than the hardness value of the as-sprayed coating (Table 3). Previous microstructural analysis of thermal spray coatings has concluded that porosity within the coating is a result of two different kinds of pore geometry, introduced by different mechanisms. One mechanism is pores formed by the expansion of trapped gases which has been previously discussed. The other mechanism is interlamellar porosity (elongated pores) at the lamellar or splat boundaries. This is believed to arise from an intermittent contact between them. Under high isostatic pressing the lamellae and splats form complete contact and hence laminar porosity is significantly reduced. It can therefore be concluded that an increase in coating hardness after HIPing at 850 °C was a result of densification within the coating which was attributed to the reduction of laminar porosity within the coating under high isostatic pressing.

4.4. HIPed at 1200 °C coated rolling elements

In the RCF testing of the coatings HIPed at 1200 °C, a very important result was obtained. In test T7, the coating of 50 μm thickness endured 70 million stress cycles without failure. In comparison with both coatings which were as-sprayed and HIPed at 850 °C, there is a significant improvement in resistance to rolling contact fatigue failure. The reason for this improvement can be related to significant changes which have occurred at the coating/substrate interface (Figs. 17–19). The location of maximum shear stress in test T7 was in the region of the coating/substrate interface. In tests on coatings of identical thickness in as-sprayed and HIPed at 850 °C state (tests T1 and T5), failure was attributed to the initiation of crack propagation as a result of the location of maximum shear stress combined with cyclic

stresses during RCF testing which led to failure by delamination after enduring less than a million stress cycles. In comparing the coating/substrate interface of the as-sprayed coating (Fig. 17) and HIPed at 1200 °C coating (Fig. 19), a number of differences were observed. At the coating/substrate interface in the as-sprayed coatings (Fig. 17) and at lower HIPing temperatures (Fig. 18), an interfacial line can be clearly seen. This interfacial line was formed by shot blasting the substrate prior to thermal spraying to improve mechanical interlock between the coating and the substrate. However, with the onset of diffusion between the coating/substrate at higher HIPing temperatures due to the Kirkendall effect, this line has been removed. It can also be seen that a number of pores have been formed within the substrate close to the interface. These are known as Kirkendall voids which are a result of the diffusion process between the coating and substrate which occurs at high HIPing temperatures. A difference in the rate of diffusion between the coating and the substrate leads to unequal fluxes of the two species from different directions. This type of unequal diffusion requires a defect mechanism. Therefore, as the substrate diffuses into the coating, an excess of vacancies are formed, which later become pores. It is therefore deduced that thermal interlocking between the coating and substrate suppressed crack propagation being initiated at the coating/substrate interface in test T7. However, it must be emphasised that further studies are required to investigate the diffusion mechanisms and crystallite phases, in order to fully appreciate this improvement at the coating/substrate interface.

In test T8 the coating endured a significant number of stress cycles before the test was automatically terminated due to an increase in vibration. Surface analysis of the wear track by SEM revealed a number of dents surrounded by a high frequency of smaller craters (Fig. 11). This type of failure was termed Denting. The larger marks have been identified as soft particle dents and result from entrapment of soft material (steel planetary balls) which deforms under the contact pressure. Entrapment of soft material occurs due to asperity contact. The R.M.S. parameter of surface roughness did not take into account peak to valley roughness. Hence, some asperities are much higher than the stated R.M.S. value which results in localised film thinning. Since the coating is essentially incompressible, the soft material forms dents in the coating since the Hertzian contact configuration and EHL film allows them no escape. The formation of a dent in full regime may locally depressurise the film resulting in a local film thinning round the dent edges. Asperity interactions occurred producing a local surface distress, which is termed a halo decorating the dent. It was therefore concluded that the increase in vibration during testing was from the high frequency of dents and surface distress within the wear track.

In test T9 the coating endured 70 million stress cycles without an increase in vibration during RCF testing. From initial surface observation, no failure in the wear track was observed (Fig. 12). However, under higher magnification a number of abrasive marks were observed within the wear track (Fig. 13). These marks were attributed to surface distress. It can be concluded that surface distress formed after a significant number of stress cycles and was a result of decreasing EHL film thickness enabling asperity contact. Depressions in the wear track, formed by high Hertzian contact load locally depressurised and thinned the lubricant film.

It is important to note that coatings HIPed at 1200 °C with a coating thickness 150 and 200 µm displayed significant improvement in resistance to rolling contact fatigue over coatings of identical thickness which were HIPed at 850 °C (Table 2). Comparison of the coating microstructure shows that at higher HIPing temperatures there is a significant increase in densification (Fig. 16). The spherical pores which were deduced to act as stress concentration points and thus initiate crack propagation, have been reduced to extremely small voids. The increase in HIPing temperature enabled hot plastic deformation as well as recrystallization to occur within the coating which led to newly formed equi-axed grains, which are very small in size due to incomplete grain growth. Combined with high Isostatic pressure the spherical pores were significantly reduced in size. Hence, the coatings HIPed at 1200 °C did not fail by delamination as a result of the improvement in microstructure which occurred at higher HIPing temperatures.

5. Conclusions

RCF tests results of HVOF coatings, deposited by JP5000 system and subjected to the post-treatment HIPing, indicate by optimising the furnace temperature of the HIPing process, it is possible to achieve over 70 million stress cycles under relative harsh contact conditions (<2 GPa) in thin coatings. This was not possible in previous investigations of thermal spray coatings, and especially not for relatively thinner (50 µm) coatings.

The microstructure of thermal spray coatings was significantly improved at elevated HIPing temperatures. At the coating/substrate interface, diffusion occurred between the coating and the substrate. This improvement in bonding enabled the 50 µm coating HIPed at 1200 °C to display significant improvement in RCF performance. Densification was significantly improved at HIPing temperatures of 1200 °C. Interlamellar porosity was eliminated by high Isostatic Pressing whilst spherical pores were reduced to micro-voids at elevated HIPing temperatures.

Results from microhardness and elastic modulus analysis not only verified increased hardness of thermal

spray coatings after HIPing but also indicated evidence of improved bonding mechanism in HIPed coatings.

Three main modes of failure were identified as delamination, denting and surface distress. Failure in as-sprayed coatings was identified as delamination and occurred in thin coatings as a result of mismatch between the coating and the substrate properties. In the coatings HIPed at 850 °C, failure was also identified as delamination and occurred in all three coating thicknesses due to cracks at the edges of pores within the microstructures acting as stress concentration points. Surface distress and denting were identified on the wear tracks of coatings HIPed at 1200 °C and were attributed to localised thinning of the lubricant film resulting in asperity contact.

6. Nomenclature

F	Contact force
H_{\min}	Minimum film thickness (μm)
P_o	Peak compressive stress (GPa)
R_{qd}	Root mean surface roughness of drive coated cone (μm)
R_{qp}	Root mean square surface roughness of driven planetary ball (μm)
A	Major axis of the contact ellipse (mm)
B	Minor axis of the contact ellipse (mm)
φ	Depth of maximum shear stress (μm)
θ	Contact angle (degrees)
ω	Spindle speed (rpm)
τ_{\max}	Maximum shear stress
λ	Non-dimensional film thickness

Acknowledgments

The authors would like to thank Dr Susan Davies at Bodycote Hot Isostatic Pressing Ltd./Infutech Ltd. for post-treatment of the coatings and Professor Rainer Gadow at the University of Stuttgart for microhardness and elastic modulus analysis. The authors also acknowledge the financial support by EPSRC (GR/R45284)

and Nuffield (NAL/00294 /G) for funding this research project.

References

- [1] S. Tobe., S. Kodama., K. Sekigushi, Conference on Proceedings of Surface Engineering International Conference, Tokyo, Japan, 1988, pp. 35–44.
- [2] S. Tobe., S. Kodama., H. Misawa, Conference on Proceedings of Thermal Spray Research and Applications, 1991, pp. 171–178.
- [3] P. Sahoo, Powder Metall. Int. 25 (1993) 73–78.
- [4] M. Hadfield., R. Ahmed., S. Tobe, Conference on Proceedings of International Thermal Spray Conference, Kobe, Japan, May 1995, pp. 1097–1102.
- [5] M. Yoshida., K. Tani., A. Nakahira, Nakajima, T. Mawatari, Thermal Spraying: Current Status and Future Trends (ITSC 95), Akira Ohmri (Ed.), Oub. High Temperature Society of Japan, Osaka University, Osaka 567, Japan, (1995), pp. 663–668.
- [6] R. Ahmed, M. Hadfield, Surf. Coat. Technol. 82 (1996) 176–186.
- [7] R. Ahmed, M. Hadfield, Wear. 203–204 (1997) 98–106.
- [8] R. Ahmed, M. Hadfield, Wear. 209 (1997) 84–95.
- [9] R. Ahmed, M. Hadfield, J. Therm. Spray Technol. 11 (2) (2002) 1–17.
- [10] F. Voort, Struct. 28 (1995) 8–13.
- [11] H. Ito, R. Nakamura., M. Shiroyama., T. Susaki, Conference on Proceedings of Thermal Spray Conference, Long Beach (CA), May 1990, pp. 20–25.
- [12] K.A. Khor, N.L. Loh, J. Therm. Spray Technol. 3 (1) (March 1994) 57–62.
- [13] H.C. Chen, E. Pfender, J. Heberlein, Thin Solid Films 293 (1997) 227–235.
- [14] K.A. Khor, Mater. Manuf. Process. 12 (2) (1997) 291–307.
- [15] K.A. Khor, Y.W. Gu, Mater. Lett. 34 (1998) 263–268.
- [16] R. Tourret, E.P. Wright, International Symposium on I. Petroleum, Heyden & Son Ltd, London, 1997, October 1976.
- [17] J. Nerz, B. Kushner, A. Rotolico, J. Therm. Spray Technol. 1 (2) (1992) 147–152.
- [18] D.C. Dunand, J. Mater. Sci. 29 (1994) 4056.
- [19] W.C. Oliver, G.M. Pharr, J. Mater. Res. 7 (1992) 1564–1583.
- [20] N.P. Suh, Wear 44 (1997) 1–16.
- [21] J.W. Flemming, N.P. Suh, Wear 44 (1977) 39–56.
- [22] N.P. Suh, N. Saka, International Conference on the fundamentals of Tribology, The MIT Press, 1980.
- [23] N.P. Suh, Prentice Hall, (1986).
- [24] P.J. Rabier, Int. J. Eng. sci. 27 (1989) 29–54.
- [25] T.E. Tallian., The American Society of Mechanical Engineers, New York, NY, 1999.